Published by
NIGERIAN SOCIETY OF PHYSICAL SCIENCES
Available online @ https://asr.nsps.org.ng/index.php/asr

African Scientific Reports 5 (2026) 422

African Scientific Reports

Geophysical investigation of groundwater potential in parts of Afao Ekiti, Southwestern Nigeria

Oladunjoye Peter Olabode*, Tokunbo Sanmi Fagbemigun, John Oluwabemiwo Olaleye, Oluwaseyi Elijah Ayobami, Tamarantare Favour Preh, Oluwatimilehin Moses Fadare

Department of Geophysics, Federal University Oye-Ekiti, P. M. B. 373, Oye-Ekiti, Ekiti State, Nigeria

Abstract

A geophysical investigation was conducted to evaluate groundwater potential and explain anomalous water-table behaviour in hand-dug wells in a new community at Afao Ekiti during the 2023–2024 dry and wet seasons. The study used water-table measurements from ten observatory wells and Vertical Electrical Soundings (VES) data acquired along five traverses with the Schlumberger array. Electrode spacing (AB/2) varied from 1 to 100 m, and the maximum surveyed length was 200 m. Water tables were higher during the dry season than during the rainy season in eight wells, while two wells remained dry in both seasons. The interpreted VES results divided the area into two zones and revealed four lithologic units: topsoil, lateritic layer, weathered layer, and fractured or fresh basement. Two aquifer types were identified: a weathered-basement unconfined aquifer with resistivity values ranging between 50–150 Ωm and a fractured-basement confined aquifer with resistivity values ranged between 100–250 Ωm. Groundwater potential is higher in Zone 1 than in Zone 2. Boreholes sited within Zone 1 are therefore expected to be productive and to yield groundwater sufficient for community needs.

DOI:10.46481/asr.2026.5.2.422

Keywords: Aquifers, Fractured basement, Groundwater potential, Vertical electrical sounding, Water table.

Article History:
Received: 18 November 2025
Received in revised form: 02 April 2026
Accepted for publication: 02 May 2026
Available online: 02 June 2026

1. Introduction

Water availability plays an important role in human societies because it is used for drinking, cooking, washing, bathing, industrial activities, and other purposes [1]. In Africa, as the human population increases, new communities are established in remote places, and adequate water supply is needed to meet their various needs. This is the case in a new community in Afao Ekiti, Ekiti State, southwestern Nigeria, where the community is experiencing anomalous water table behaviour in its water supply. This anomalous behaviour of the water table in the locality has raised scientific concerns that need to be investigated. The Department of Geophysics, Federal University Oye-Ekiti, was asked to investigate why a rise in water tables in wells during the dry season, compared with a fall in water tables during the wet season, affects the community water supply. The confined and unconfined aquifer characteristics

*Corresponding author Tel. No.: +234 803-257-8542
Email address: oladunjoye.olabode@fuoye.edu.ng (Oladunjoye Peter Olabode)

within the subsurface geology of the study area may be responsible for this effect of hydrogeological conditions on the water table [2], and these characteristics can be investigated with the electrical resistivity method.

The electrical resistivity method is useful for delineating areas suitable for groundwater abstraction that is not strongly affected by seasonal variation. Electrical resistivity has been found effective in the search for geological structures that can accumulate or store water because it responds to the fluid content of subsurface materials [3]. The electrical resistivity technique of Vertical Electrical Sounding (VES) is widely adopted in crystalline basement terrain for delineating fractured or weathered basement associated with the weathering of crystalline rock [4–6]. It has been adopted by several researchers to investigate groundwater potential and delineate aquifer units for groundwater development in crystalline basement terrain. Ref. [7] carried out a geophysical survey using the VES technique to delineate the subsurface geoelectric characteristics of the basement complex and evaluate groundwater potential at Annunciation Grammar School, Ikere Ekiti, southwestern Nigeria. Ref. [8] carried out a more detailed study by combining Very Low Frequency - Electromagnetic (VLF-EM) and VES methods to evaluate the groundwater potential of the Innovation Area of Phase One, Federal University Oye-Ekiti. The VLF-EM profiles delineated linear geologic structures and served as a guide for locating VES stations. Recently, Ref. [9] used VES for groundwater exploration in parts of the crystalline basement complex terrain of Nigeria to delineate the geoelectrical characteristics of the subsurface geology.

This study measures the water table in observatory wells to obtain water-table depths in the weathered-basement unconfined aquifer zone. It also uses VES with the Schlumberger array configuration to provide subsurface geoelectric information on the underlying geology and its groundwater capacity in the confined aquifer, which can yield substantial groundwater and may not be affected by seasonal variation.

1.1. Location of the study

The study site is a new community in Afao Ekiti, Ekiti State (Figure 1). It is situated along the Afao–Ire–Iworoko Ekiti Road. The study area is gently undulating from east to west and is bounded by a stream that flows from north to west, crossing the Afao–Ire–Iworoko Ekiti Road. Both the road and the stream are outside the studied area.

The area is underlain by the Precambrian Basement Complex of Southwestern Nigeria, which is composed of the migmatite–gneiss complex with granite–gneiss lithologic units [10], as shown in Figure 2. The area is located within the tropical rainforest zone and receives annual rainfall above 1367 mm.

2. Materials and methods

The investigation involved measuring the water table in ten observatory hand-dug wells in the community during the wet season, from May to June 2023, and during the dry season, from December 2023 to January 2024. A measuring sonde was lowered into each well until it touched the water and produced a sound. The depth scale was read at ground level to determine the water table. The distance from the ground surface to the water in the well was recorded as the water-table depth.

The electrical resistivity method, using the VES technique with the Schlumberger electrode configuration, was adopted for data acquisition in the study location. Four steel electrodes were used: two electrodes measured potential difference, while two electrodes transmitted current into the ground. The two potential electrodes were positioned between the two current electrodes. The current electrodes were expanded from 1 to 100 m from the potential electrodes at the centre of the survey, with the four electrodes arranged collinearly. An Ohmega digital resistivity meter was used for data collection. Five profiles were established within the community, and VES stations were occupied along these profiles. Thirty-two VES data sets were acquired using the Schlumberger array with electrode spacing varing from 1 to 100 m. The VES curves were interpreted quantitatively using partial curve matching and computer-assisted forward modelling with WinResist software.

The kriging interpolation method was adopted to generate the maps. This approach examines the spatial distribution of the data and fits a mathematical model to the sample data to determine spatial autocorrelation, which is then used to predict or estimate values at unsampled locations. The result was validated using the standard error for estimation accuracy.

3. Results and discussion

3.1. Observatory wells

Preliminary results of water-table measurements in hand-dug wells within the study location for two months in May and June 2023 are shown in Table 1. Three of the ten observatory wells (wells 7, 8, and 10) were dry during this period, although it was the rainy season, whereas the remaining seven wells (wells 1, 2, 3, 4, 5, 6, and 9) contained water. Statistical analysis of the data showed an increase in water table in four wells (wells 3, 4, 6, and 9) from the first measurement in Week 1. The weather conditions were rainy in Weeks 2 and 3, humid in Weeks 1 and 4, and sunny in Week 5.

Table 2 shows the results of water-table measurements taken during the dry-season period in December and January. The water table increased in most of the observatory wells during the dry season. Eight of the ten observatory wells (wells 1, 2, 3, 4, 5, 6, 7, and 9) contained water, whereas wells 8 and 10 were dry. Comparing Tables 1 and 2 shows a corresponding increase in water table during the dry season compared with the wet season.

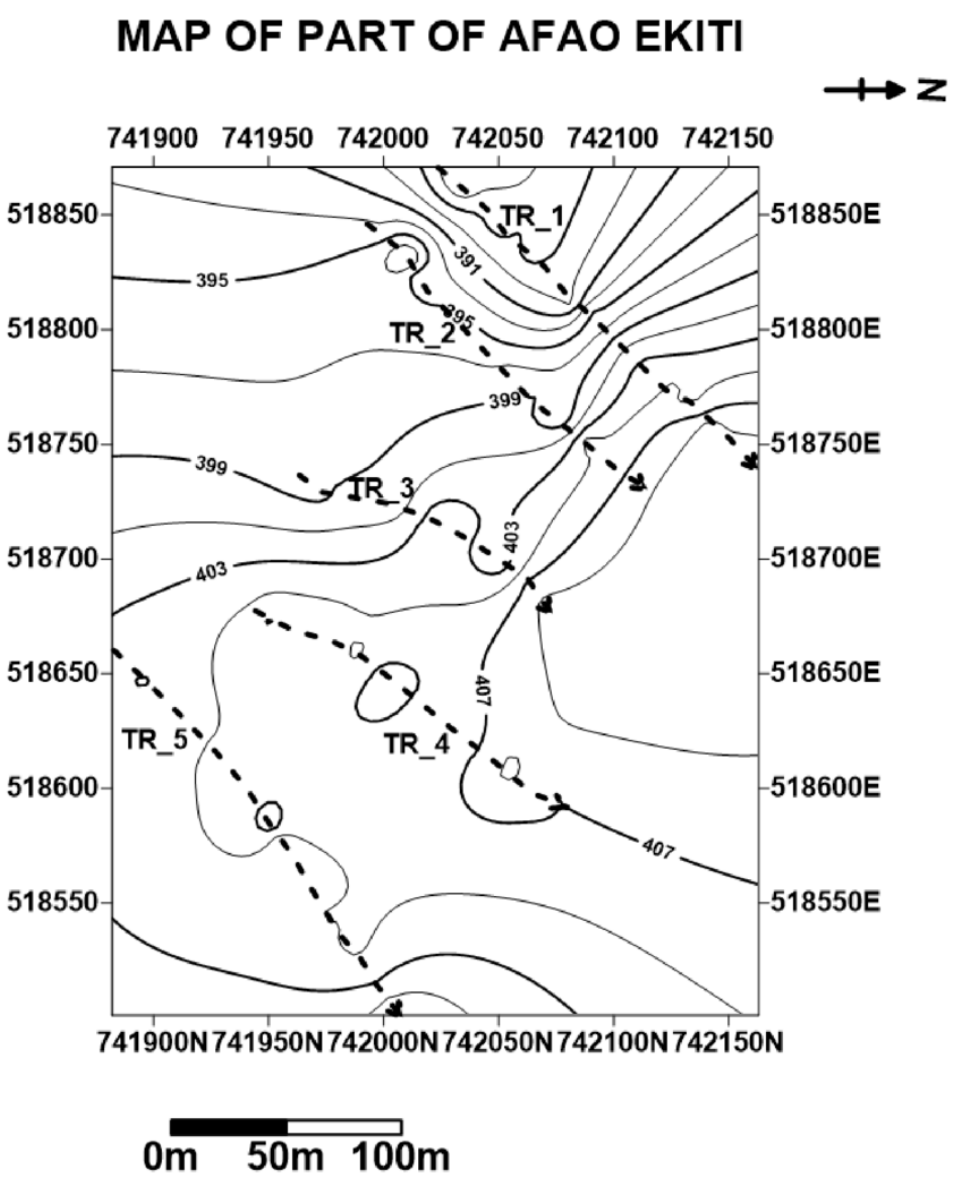

Figure 1: Topographical map of part of Afao Ekiti showing traverse lines and directions.

3.2. VES data interpretation

Table 3 summarizes the 32 VES data sets. The interpretation revealed four geoelectric units, interpreted as lithologies in the study site: topsoil, lateritic layer, weathered layer, and fractured or fresh basement. The model results also revealed two curve types: 16 K-type curves and 16 KH-type curves. However, the surveyed area may be dominated by KH-type curves if the surveyed lengths of the delineated K-type curves were not affected by barriers during data acquisition. Typical VES curves in the study area are shown in Figure 3. The figure presents two K-type curves from Traverse 5 VES 2 and Traverse 1 VES 4, and two KH-type curves from Traverse 2 VES 1 and Traverse 5 VES 1. The resistivity distribution ranged from 8.6 Ωm in VES 3 to 11070.3 Ωm in VES 2. The topsoil resistivity distribution ranged from 31.1 Ωm in VES 27 to 316.7 Ωm in VES 20. The lateritic layer, which forms a hardpan and is widely exposed in the study site, had resistivity values ranging from 229.3 Ωm in VES 11 to 2299.6 Ωm in VES 12. The lowest resistivity values were obtained in the weathered layer, ranging from 8.6 to 164.0 Ωm in VES 3 and VES 21, respectively. The fractured or fresh basement resistivity values ranged from 109.5 Ωm in VES 5 to 11070.3 Ωm in VES 2. The layer thickness and depth to bedrock ranged from 0.4 to 28.8 m in VES 21, VES 25, VES 27, and VES 5, and from 4.8 to 38.8 m in VES 11 and VES 3, respectively.

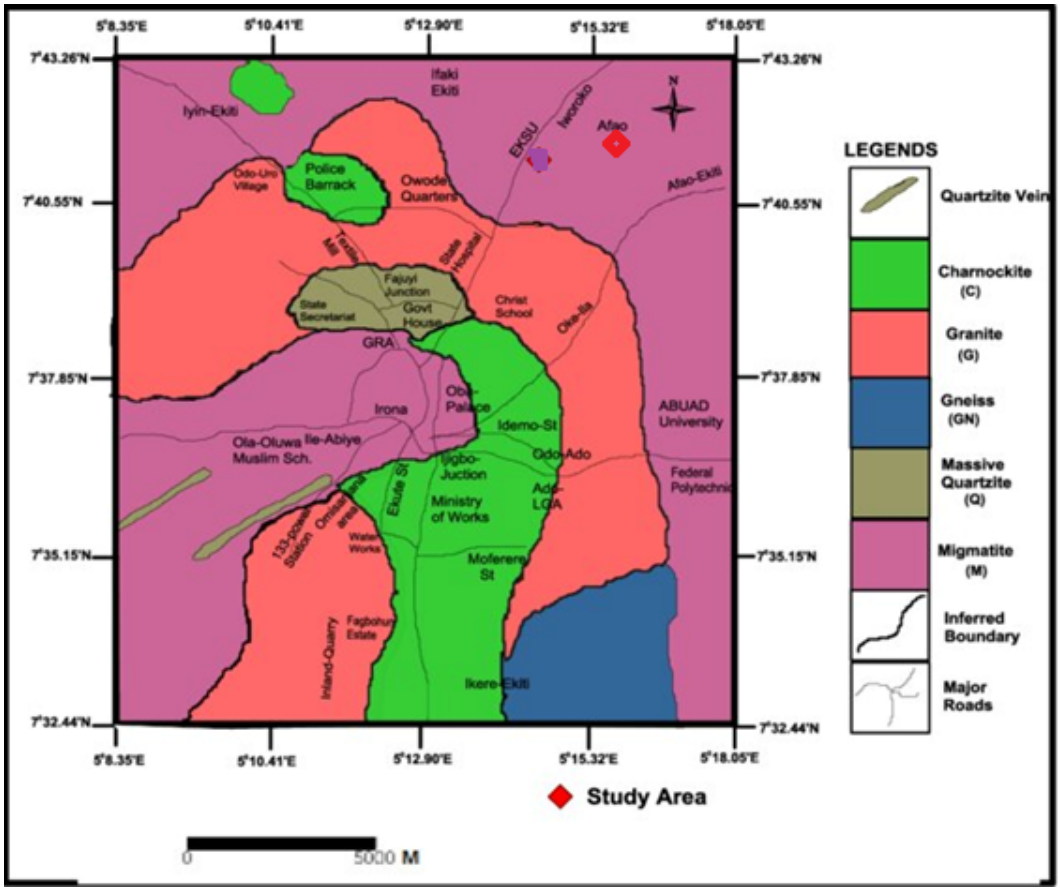

Figure 2: Geological map of Ado Ekiti (modified after Ref. [10]).

Table 1: Water-table measurement results in the wet season.

Well no.	Type	Week 1 (May 5) Depth (m)	Week 2 (May 12) Depth (m)	Week 3 (May 19) Depth (m)	Week 4 (May 26) Depth (m)	Week 5 (June 2) Depth (m)	Mean
1	Wet	6.58	6.85	6.67	6.67	6.74	6.702
2	Wet	8.10	8.68	8.28	8.33	8.26	8.330
3	Wet	15.10	15.03	13.64	15.10	15.40	14.854
4	Wet	8.20	7.03	6.56	6.64	6.70	7.026
5	Wet	8.27	7.83	8.38	8.37	8.59	8.288
6	Wet	8.81	8.32	8.33	8.23	8.50	8.438
7	Dry	Dry	Dry	Dry	Dry	Dry	–
8	Dry	Dry	Dry	Dry	Dry	Dry	–
9	Wet	13.20	13.08	12.99	13.10	13.13	13.100
10	Dry	Dry	Dry	Dry	Dry	Dry	–
Weather condition		Humid	Rainy	Rainy	Humid	Sunny	

3.3. Isopach maps of the study site

Figure 4 shows the distribution of topsoil thickness, which ranged from 0.4 to 2.5 m in the study location. Topsoil with an average thickness of 0.85 m was observed from the centre towards the western part of the map, whereas the southern and northeastern parts recorded higher thicknesses greater than 1.3 m. Laterite outcrops were observed in the central and western parts of the mapped area.

Figure 5 shows the distribution of weathered-layer thickness, which ranged from 15 m in the west to 31 m in the south. Average thicknesses greater than 21 m were observed from the north through the centre towards the southern part of the mapped area, except in the western and eastern parts, where thicknesses were less than 21 m. The weathered layer is fairly thick in the south and becomes progressively thicker towards the north of the mapped area.

Table 2: Water-table measurement results in the dry season.

Well no.	Type	Week 1 (Dec. 1) Depth (m)	Week 2 (Dec. 14) Depth (m)	Week 3 (Dec. 21) Depth (m)	Week 4 (Dec. 29) Depth (m)	Week 5 (Jan. 5, 2024) Depth (m)	Mean
1	Wet	5.68	4.58	4.84	5.78	4.95	5.166
2	Wet	7.81	8.10	7.88	8.02	7.98	7.960
3	Wet	13.55	14.67	14.64	13.11	13.45	13.884
4	Wet	7.05	5.73	5.86	5.47	5.97	6.016
5	Wet	7.87	7.23	7.68	7.17	7.89	7.568
6	Wet	8.01	7.82	7.53	7.73	7.51	7.720
7	Wet	12.99	13.01	12.95	12.98	13.03	12.992
8	Dry	Dry	Dry	Dry	Dry	Dry	–
9	Wet	12.51	12.84	12.12	12.61	12.63	12.542
10	Dry	Dry	Dry	Dry	Dry	Dry	–

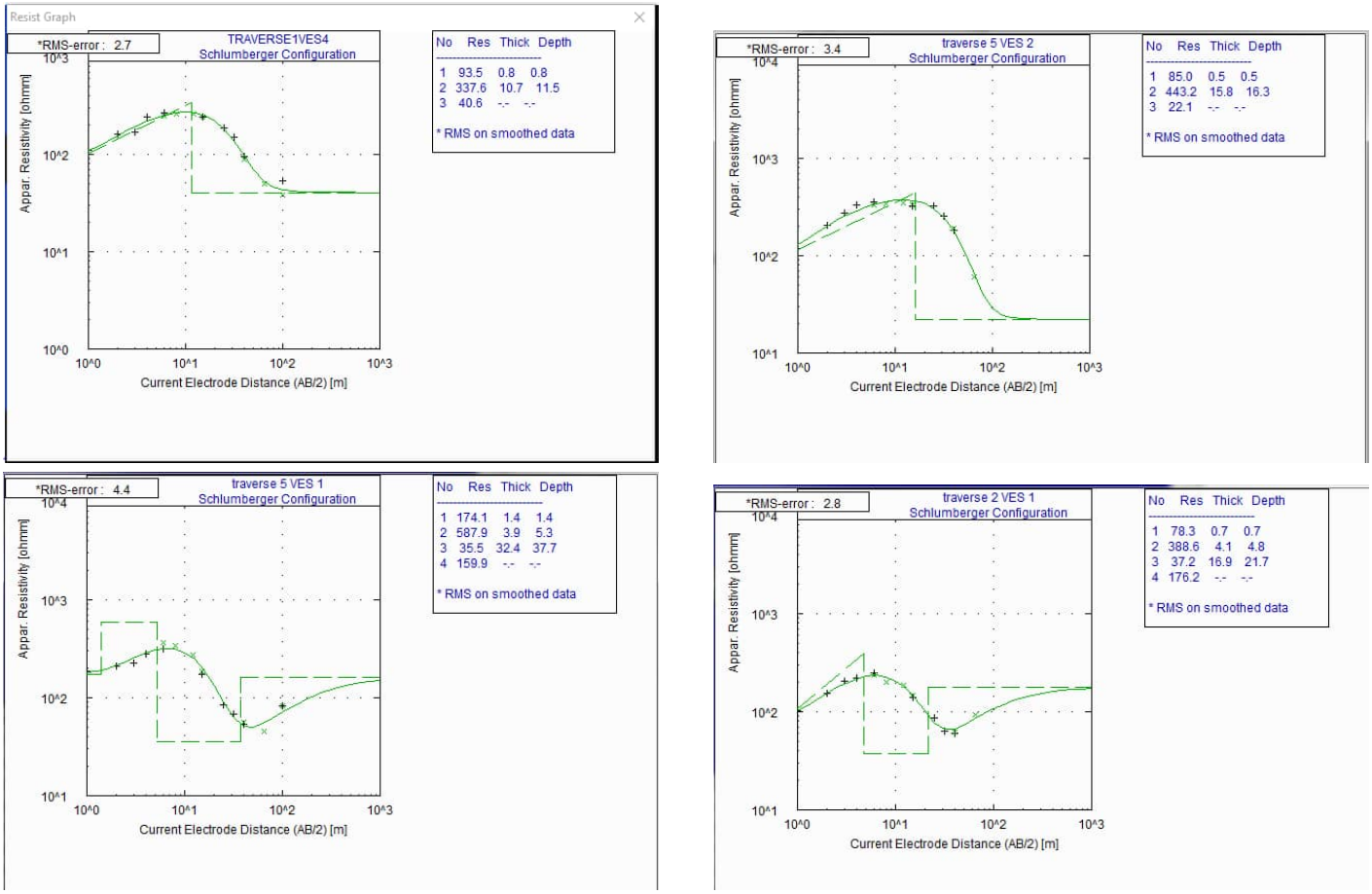

Figure 3: Typical VES curves showing (A) K-type curves and (B) KH-type curves in the study area.

3.4. Iso-resistivity maps of the study site

Figure 6 shows the subsurface resistivity distribution of the topsoil in the study location. The resistivity values ranged from 70 Ωm in the south to 270 Ωm in the north. The average resistivity value across the mapped area is about 150 Ωm.

Figure 7 shows the subsurface resistivity distribution of the weathered layer in the study location. The resistivity values ranged from less than 35.0 Ωm in the southeast and northwest to more than 140.0 Ωm in the centre of the mapped area. Resistivity values greater than 50.0 Ωm occupied the area from the north through the centre to the south, suggesting groundwater potential because weathered granite with resistivity values greater than 50 Ωm and a fairly thick profile can yield reasonable groundwater [11]. The mapped area can be divided into two zones: Zone 1, occupied by resistivity values greater than 50 Ωm, and Zone 2, occupied by resistivity values less than 50 Ωm.

Table 3: Summary of the VES interpretation results.

VES no.	Traverse no.	Curve type	Layers	Resistivity (Ωm)	Thickness (m)	Depth (m)	Lithology
				125.6	0.7		Topsoil
				1181.9	3.7	0.7	Lateritic layer
				39.3	19.7	4.4	Weathered layer
1	1	KH	4	5977.3	–	24.1	Basement
				69.6			Topsoil
				273.5	0.6	0.6	Lateritic layer
				20.4	5.2	5.8	Weathered layer
2	1	KH	4	11070.3	12.9	18.7	Basement
				144.9			Topsoil
				300.7	0.6	0.6	Lateritic layer
				8.6	10.6	11.2	Weathered layer
3	1	KH	4	1130.8	22.6	33.8	Basement
				93.5			Topsoil
				337.6	0.8	0.8	Lateritic layer
4	1	K	3	40.6	10.7	11.5	Weathered layer
				103.2	0.6		Topsoil
				779.6	4.4	0.6	Lateritic layer
				38.5	28.8	5.0	Weathered layer
5	1	KH	4	109.5	–	38.8	Fractured basement
				101.4	0.7	0.7	Topsoil
				511.8	9.5	10.2	Lateritic layer
				10.5	19.9	30.1	Weathered layer
6	1	KH	4	293.8	–	–	Basement
				117.7	0.9	0.9	Topsoil
				406.8	10.8	11.7	Lateritic layer
				25.8	18.3	30.0	Weathered layer
7	1	KH	4	652.7	–	–	Basement
				123.1			Topsoil
				1033.8	1.3	1.3	Lateritic layer
8	1	K	3	22	11.1	12.4	Weathered layer
				120.9	1.2		Topsoil
				1487.4	9.8	1.2	Lateritic layer
9	1	K	3	35.4	–	11.0	Weathered layer
				78.3	0.7	0.7	Topsoil
				388.6	4.1	4.8	Lateritic layer
				37.2	16.9	21.7	Weathered layer
10	2	KH	4	176.2	–	–	Fractured basement
				72.4			Topsoil
				229.3	0.7	0.7	Lateritic layer
11	2	K	3	38.1	4.1	4.8	Weathered layer

3.5. Columnar section beneath VES points

Figure 8 illustrates the geoelectric layers in vertical succession beneath VES 3, VES 10, VES 15, VES 22, and VES 30 in Traverses 1, 2, 3, 4, and 5, respectively. The columnar section was generated across the mapped area in a west–east direction passing through the five traverses. The topsoil is the uppermost geoelectric layer and has a very thin thickness and moderate resistivity values, as observed in the isopach map (Figure 4) and iso-resistivity map (Figure 6), respectively. This is followed by the lateritic layer, which is relatively thick and has higher resistivity values. The weathered layer is the third geoelectric unit. It is relatively thicker than the lateritic layer and has lower resistivity values. The resistivity values beneath VES 3 and VES 30 are less than 10 Ωm in Traverses 1 and 5, respectively. The resistivity values of the weathered layer beneath VES 10, VES 15, and VES 22 are greater than 10 Ωm but less than 50 Ωm. Wells located close to Traverses 2, 3, and 4 are rarely affected by anomalous changes in the water table during the dry and wet seasons compared with wells located around Traverses 1 and 5. The fourth geoelectric unit is the fractured or fresh basement. The resistivity value beneath VES 3 is 1130.8 Ωm, indicating fresh basement. However, the low resistivity values beneath VES 10, VES 15, and VES 30 are 176.2, 267.7, and 199 Ωm, respectively, suggesting water-saturated fractured basement. Boreholes sited within this zone (Zone 1) are expected to be productive and to yield groundwater that can serve community needs.

Table 3: Summary of the VES interpretation results (continued).

VES no.	Traverse no.	Curve type	Layers	Resistivity (Ωm)	Thickness (m)	Depth (m)	Lithology
				154	1.5	1.5	Topsoil
				2299.6	7.0	8.5	Lateritic layer
12	3	K	3	84.3	–	–	Weathered layer
				158.6			Topsoil
				2178.9	0.7	0.7	Lateritic layer
13	3	K	3	164.8	5.4	6.1	Weathered layer
				301.4			Topsoil
				949.2	0.5	0.5	Lateritic layer
14	3	K	3	71.8	11.3	11.8	Weathered layer
				126.2			Topsoil
				308.4	1.3	1.3	Lateritic layer
				20.0	11.7	13.0	Weathered layer
15	3	KH	4	267.7	18.3	31.3	Basement
				256.9			Topsoil
				1142.7	1.8	1.8	Lateritic layer
16	3	K	3	66.5	10.0	11.8	Weathered layer
				35.1			Topsoil
				1803.8	0.5	0.5	Lateritic layer
				25.9	4.2	4.7	Weathered layer
17	3	KH	4	130.4	26.6	31.3	Fractured basement
				78.3			Topsoil
				1209.2	0.6	0.6	Lateritic layer
18	3	K	3	74.7	5.6	6.2	Weathered layer
				186.1			Topsoil
				1400.1	0.6	0.6	Lateritic layer
19	3	K	3	84.6	4.4	5.0	Weathered layer
				316.7			Topsoil
				1050.1	1.7	1.7	Lateritic layer
20	3	K	3	81.3	10.0	11.7	Weathered layer
				213.3			Topsoil
				882.8	0.4	0.4	Lateritic layer
21	4	K	3	116.0	11.9	12.3	Weathered layer
				146.0			Topsoil
				549.0	1.3	1.3	Lateritic layer
22	4	K	3	40.4	13.8	15.1	Weathered layer

3.6. Depth to bedrock

Figure 9 shows the map of subsurface regolith-thickness distribution and bedrock relief in the study site. The regolith thickness ranged from 21 m in the west to 39 m in the centre of the study area. It is shallowest in the western part and becomes progressively deeper towards the centre, with an average depth greater than 29 m. The contour lines are evenly spaced, suggesting a uniform slope with a gently sloping surface. Therefore, the bedrock relief is gently undulating from west to east across the mapped area.

3.7. Discussion of results

The resistivity values ranging between 50–150 Ωm for the weathered layer on the iso-resistivity map (Figure 7) and 100–250 Ωm for the fractured basement in the columnar section (Figure 8) fall within Zone 1, extending from the north through the centre towards the south of the study area, and constitute the aquifers in the study location. Zone 1 has thickness greater than 21 m, as observed in the isopach map of the weathered layer (Figure 5). Because the aquifer in Zone 1 is considerably thick, with thickness greater than 21 m, resistivity values greater than 50 Ωm for weathered granite, and resistivity values generally lower than 200 Ωm for fractured basement, the groundwater potential is high in Zone 1. Resistivity values less than 50 Ωm observed in Zone 2 with thickness less than 21 m may be interpreted as clay material within the weathered granite [11]. This massive clay was encountered in VES 3 and VES 6 of Traverse 1, with resistivity values of 8.6 and 10.5 Ωm, respectively (Figure 6 and Table 3). In Traverse 5, clay was encountered in VES 30 with a resistivity value of 9.4 Ωm (Figure 8 and Table 3). This information corroborates the results obtained from the observatory wells (Tables 1 and 2) because wells sited in Zone 2, where these clay materials are deposited, experienced dryness in

Table 3: Summary of the VES interpretation results (continued).

VES no.	Traverse no.	Curve type	Layers	Resistivity (Ωm)	Thickness (m)	Depth (m)	Lithology
23	5	KH	4	174.1 587.9 35.5 159.9	1.4 3.9 32.4 –	1.4 5.3 37.7 –	Topsoil Lateritic layer Weathered layer Fractured basement
24	5	K	3	85 443.2 22.1	0.5 15.8 –	0.5 16.3 –	Topsoil Lateritic layer Weathered layer
25	5	KH	4	114.3 342.5 40.4 407.3	0.4 9.3 20.9 –	0.4 9.7 30.6 –	Topsoil Lateritic layer Weathered layer Basement
26	5	KH	4	96 398.9 38.6 1103.1	0.5 12.9 16.4 –	0.5 13.4 29.8 –	Topsoil Lateritic layer Weathered layer Basement
27	5	KH	4	31.1 2251.4 30.1 272	0.4 3.6 23.4 –	0.4 4.0 27.4 –	Topsoil Lateritic layer Weathered layer Basement
28	5	KH	4	59.4 743.2 36.3 840.4	0.6 7.9 20.8 –	0.6 8.5 29.3 –	Topsoil Lateritic layer Weathered layer Basement
29	5	KH	4	160.2 303.7 61.7 133.8	1.0 6.9 19.6 –	1.0 7.9 27.5 –	Topsoil Lateritic layer Weathered layer Fractured basement
30	5	KH	4	178.8 314.7 9.4 199	1.0 7.9 18.8 –	1.0 8.9 27.8 –	Topsoil Lateritic layer Weathered layer Fractured basement
31	5	K	3	235.9 328.4 40.5	2.5 3.9 –	2.5 6.4 –	Topsoil Lateritic layer Weathered layer
32	5	K	3	208.8 319.6 55.8	1.7 4.5 –	1.7 6.2 –	Topsoil Lateritic layer Weathered layer

most seasons, whereas wells sited in Zone 1 of the study area are usually wet in all seasons because of the high groundwater potential in this zone.

Groundwater flow is influenced by several factors, such as gravity, pressure, geology, topography, and permeability [12, 13]. These factors are responsible for groundwater flow in this study because groundwater flows from areas of shallow depth in the west of the mapped area to deeper areas in the centre under the influence of gravity, fresh-basement topography or relief, hydraulic pressure, and formation geology, particularly aquifer type (Figure 9). The basement depression observed in the centre of the depth-to-basement map and in the columnar section around Traverses 3 and 4 (Figures 8 and 9) serves as a reservoir or basin for collecting groundwater flow. As rainwater percolates into the subsurface during rainfall events through pore spaces, it encounters clay materials, which hydrate and swell as they absorb water. Clay materials generally swell when hydrated and shrink as they lose water during drying [14]. Therefore, the reduction in hydraulic heads in the observatory wells during the rainy season and the consequent increase during the dry season may be due to clay minerals absorbing water during the rainy season and losing water from their structures to the surroundings during the dry season. The major factor influencing groundwater flow in this study can be related to groundwater recharge and discharge, which may affect water-table depths [12]. The groundwater potential of the study site is very high and will support considerable groundwater yield, especially in Zone 1, which can serve community needs.

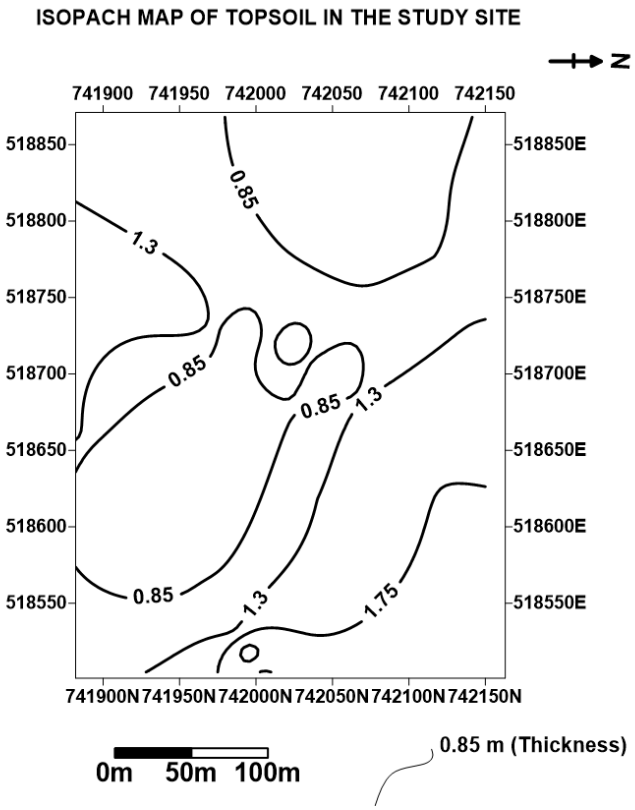

Figure 4: Isopach map of the topsoil in the study site showing its thickness.

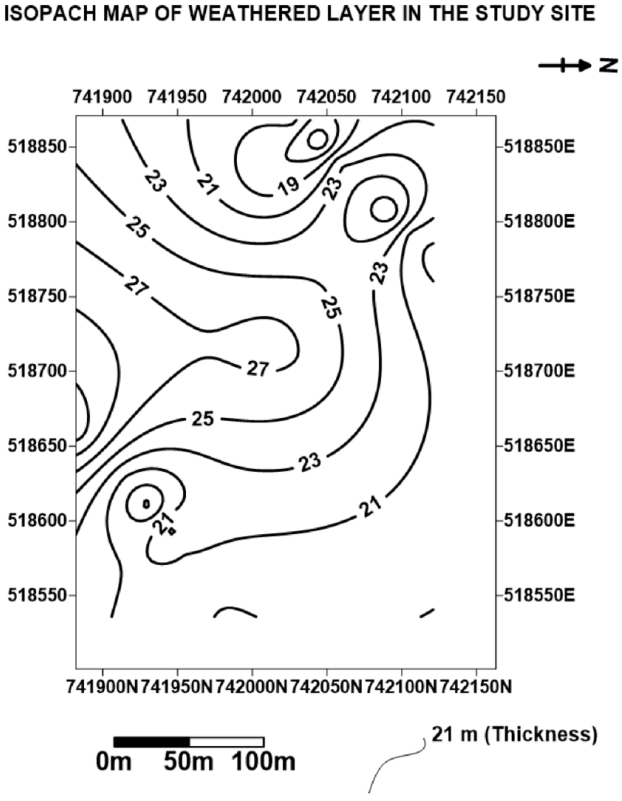

Figure 5: Isopach map of the weathered layer in the study site showing its thickness.

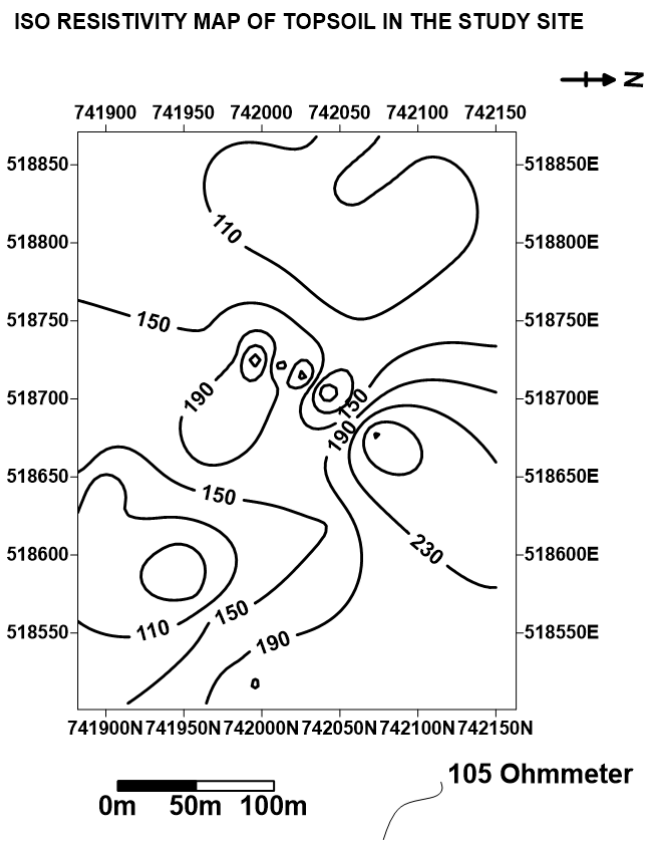

Figure 6: Iso-resistivity map of the topsoil in the study site showing its subsurface resistivity distribution.

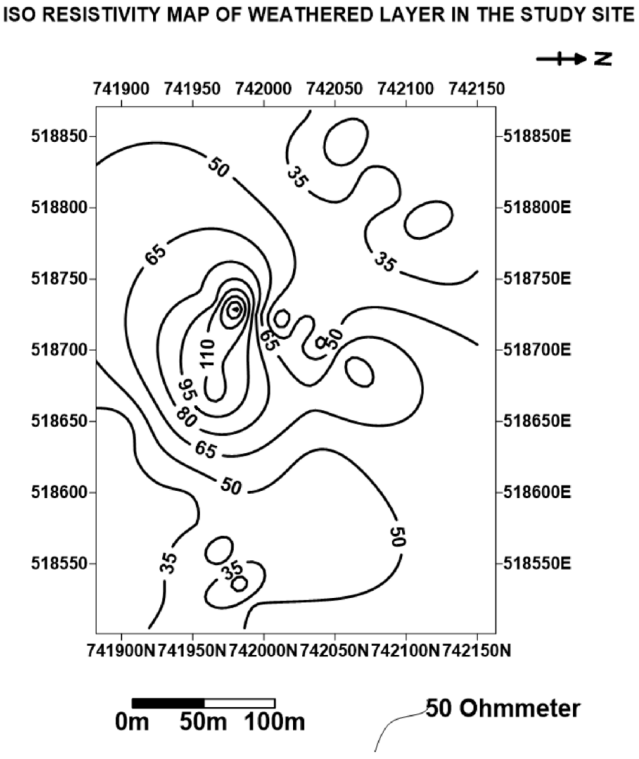

Figure 7: Iso-resistivity map of the weathered layer in the study site showing its subsurface resistivity distribution.

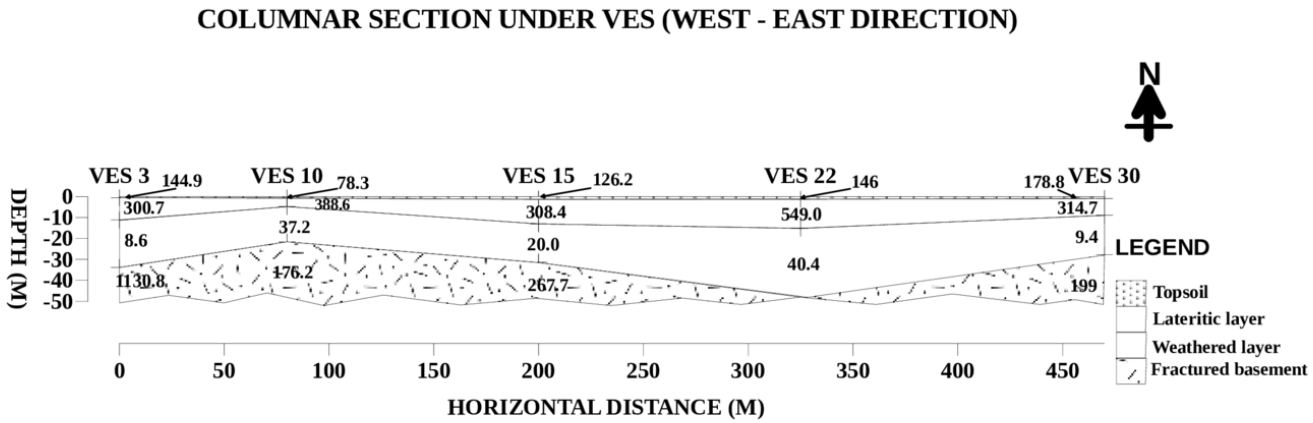

Figure 8: Columnar sections showing the resistivity values of geoelectric layers in vertical succession beneath selected VES points.

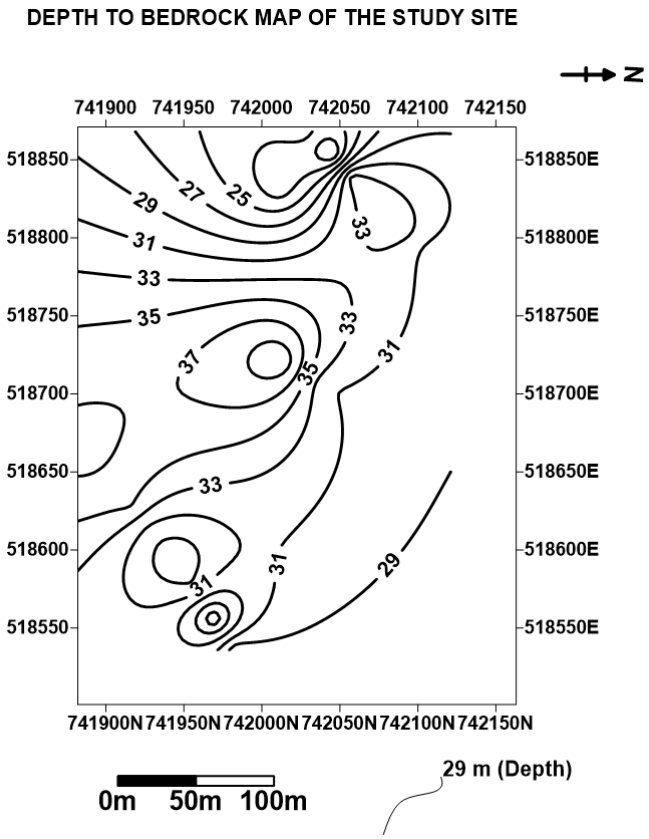

Figure 9: Depth-to-bedrock map of the study site showing the subsurface regolith thickness distribution and bedrock relief.

4. Conclusion

This geophysical investigation of groundwater potential was carried out to assess the groundwater potential of the study area and suggest an alternative water-supply source based on the geoelectric properties of the layered subsurface geology. The results show that the groundwater potential of the study site is high, especially in Zone 1, within the main aquifer, which is the fractured basement in the study area. Borehole siting and groundwater abstraction should be restricted to the fractured basement within Zone 1 of the study location. Groundwater flow influences recharge and discharge in the study area and causes changes in water-table depths.

Data availability

Data will be made available on request.

Declaration of competing interest

The authors declare that they have no known competing financial interests or personal relationships that could have appeared to influence the work reported in this manuscript.

Funding

The authors received no external funding for this study.

Acknowledgment

The authors thank the undergraduate students who assisted with fieldwork during data acquisition. Support from the Department of Geophysics, Federal University Oye-Ekiti, and various parties is gratefully acknowledged.

References

[1] K. E. Welsh & A. P. Pinder-Darling, “Water availability and access”, in Clean Water and Sanitation, W. Leal Filho, A. M. Azul, L. Brandli, A. Lange Salvia & T. Wall (Eds.), Springer, Cham, Switzerland, 2022, p. 736. https://doi.org/10.1007/978-3-319-95846-0_165.

[2] Z. Liu, Y. Zhang, Z. Guan, J. Li & Y. Huang, “Impact of hydrogeological conditions on groundwater vulnerability in the Songnen Plain, Jilin, China”, LHB: Hydroscience Journal **111** (2025) 2579898. https://doi.org/10.1080/27678490.2025.2579898.

[3] R. M. Hen-Jones, P. N. Hughes, R. A. Stirling, S. Glendinning, J. E. Chambers, D. A. Gunn & Y. J. Cui, “Seasonal effects on geophysical–geotechnical relationships and their implications for electrical resistivity tomography monitoring of slopes”, Acta Geotechnica **12** (2017) 1159. https://doi.org/10.1007/s11440-017-0523-7.

[4] M. O. Olorunfemi, J. O. Fatoba & L. O. Ademilua, “Integrated VLF-electromagnetic and electrical resistivity survey for groundwater in a crystalline basement complex terrain of Southwest Nigeria”, Global Journal of Geological Sciences **3** (2005) 71. https://doi.org/10.4314/gjgs.v3i1.18714.

[5] O. P. Olabode, J. T. Fatoba & S. O. Ariyo, “Combined VLF-EM and geoelectric sounding for groundwater development in a typical basement complex terrain of Southwestern Nigeria”, FUW Trends in Science & Technology Journal **2** (2017) 496. Available online: https://www.researchgate.net/publication/319154055.

[6] O. P. Olabode & A. Adeniji, “Application of electrical resistivity in evaluating a section of road conditions–a case study in Ifaki-Oye-Ikole Ekiti Highway, Nigeria”, Arabian Journal of Geosciences **15** (2022) 1169. https://doi.org/10.1007/s12517-022-10449-z.

[7] T. A. Lateef, “Geophysical investigation for groundwater using electrical resistivity method–a case study of Annunciation Grammar School, Ikere LGA, Ekiti State, Southwestern Nigeria”, IOSR Journal of Applied Physics **2** (2012) 1. https://doi.org/10.9790/4861-0210106.

[8] O. P. Olabode, K. B. Osayomi & O. Bamidele, “Evaluation of groundwater potential of part of Phase One, Federal University Oye-Ekiti using electromagnetics and electrical resistivity methods”, FUOYE Journal of Pure and Applied Sciences **3** (2019) 334. Available online: https://fjpas.fuoye.edu.ng/index.php/fjpas/article/view/92.

[9] O. Fawale, T. O. Lawal & J. S. Abayomi, “A geo-electrical survey for groundwater exploration in a part of the Basement Complex terrain, Ilorin Metropolis, Northcentral Nigeria”, Nigerian Journal of Physics **32** (2023) 55. Available online: https://njp.nipngr.org/index.php/njp/article/view/50.

[10] C. A. Ajayi, H. Y. Madukwe, S. O. Ilugbo, B. A. Adebo, A. O. Talabi, A. A. Oyedele, O. F. Ojo, Y. C. Ajisafe & J. I. Talabi, “Geophysical investigation of post-foundation assessment within Ekiti State University, Ado Ekiti, Southwestern Nigeria”, Malaysian Journal of Geosciences **6** (2022) 88. https://doi.org/10.26480/mjg.02.2022.88.96.

[11] J. M. Reynolds, “The role of surface geophysics in the assessment of regional groundwater potential in Northern Nigeria”, Geological Society, London, Engineering Geology Special Publications **4** (1987) 185. https://doi.org/10.1144/GSL.ENG.1987.004.01.22.

[12] F. Meng, C. Xiao, X. Liang, G. Wang, Y. Sun & D. Guo, “Factors influencing surface water and groundwater interaction in alluvial fan”, Journal of Water and Climate Change **12** (2021) 679. https://doi.org/10.2166/wcc.2020.174.

[13] B. Li, Y.-F. Zeng, B.-B. Zhang & X.-Q. Wang, “A risk evaluation model for karst groundwater pollution based on geographic information system and artificial neural network applications”, Environmental Earth Sciences **77** (2018) 334. https://doi.org/10.1007/s12665-018-7539-7.

[14] E. Kalkan, “Impact of wetting–drying cycles on swelling behavior of clayey soils modified by silica fume”, Applied Clay Science **52** (2011) 345. https://doi.org/10.1016/j.clay.2011.03.014.